Robotics and Autonomous Systems 125 (2020) 103427

Contents lists available at ScienceDirect

Robotics and Autonomous Systems

journal homepage: www.elsevier.com/locate/robot

A dual-mode soft gripper for food packaging

Zhongkui Wang *, Keung Or, Shinichi Hirai

Soft Robotics Laboratory, Department of Robotics, Ritsumeikan University, 525-8577 Noji-Higashi 1-1-1, Kusatsu, Shiga, Japan

ARTICLE INFO

Article history:
Received 17 February 2019
Received in revised form 4 December 2019
Accepted 6 January 2020
Available online 11 January 2020

Keywords:
Soft gripper
Grasping
Suction
Food packaging
Automation

ABSTRACT

Robotics and automation in the food industry is not as widely applied as in other industries, such as automotive and electrical industries, due to the large variations in the shape and properties of food materials and the frequent alterations of food products. Robotic end effectors that can adapt to these variations and handle multiple types of food materials are in high demand. Therefore, we propose a dual-mode soft gripper made of rubber material that can grasp and suck different types of objects. The gripper consists of four soft fingers, fabricated with rubber material using casting process, each of which is designed as a combination of a PenuNet bending actuator and a suction pad located at the fingertip. We introduce a new design for the air paths, which play an important role in the proper function of the soft finger. Finite element (FE) simulations were performed to confirm the finger design. Experimental tests were conducted to evaluate single finger bending, gripper lifting force, and grasping and sucking actions for various types of food materials. Results show that the soft gripper can lift a 273.97-g hot dog in the grasping mode, as well as a 512.62-g bagged Kernel corn and a 1072.65-g Macbook Air in the suction mode. It can adapt to approximately circular and square targets, such as a piece of fried chicken and an orange, when the soft fingers are in a perpendicular configuration. While in a parallel configuration, the gripper can successfully handle elongated targets, such as a hot dog. An experiment is also presented to demonstrate the automatic packaging of a Japanese boxed lunch, which requires both grasping and suction modes to be employed.

1. Introduction

In the last two or three decades, factory automation (FA) has undergone extensive developments and industrial robots are now widely utilized in most processes within automotive and electrical industries. However, contrary to expectation, FA is not frequently employed in fields such as light industry, agriculture, the forestry and fisheries industry, the food industry, medicine, cosmetics, clothing, and packaging [1]. These fields pose various difficulties and challenges for the development of new robots; for example, how to handle and adapt to the deformity, fragility, individual differences, and complex surface properties of the target objects. Specific challenges also include robot portability, ease of use for amateurs, reduction of system weight and cost, and improving the safety of human–robot interaction.

In the last decade, the emerging research field of soft robotics has shown substantial potential for solving some of the above-mentioned problems. Making robot using soft materials, which are typically light weight, can solve the heavy weight problem. Deformable robots can cope with the deformities and individual differences of target objects. This can then simplify the control system because the soft robot body accommodates some of the control work, which is characterized by morphological computation [2]. As a result, the robotic system can be simplified and the system cost can be reduced. Lastly, soft materials can absorb impact energy during contact with the environment, which increases their safety.

In this study, we focus on soft robotic gripper for handling food materials. According to a recent review [3], soft robotic grippers can be categorized into three groups based on grasping principle: (1) gripping by actuation, (2) gripping by controlled stiffness, and (3) gripping by controlled adhesion. Most grippers in the first and second groups use static friction to lift objects, such as the grippers based on soft pneumatic actuators [4,5], the MR fluid gripper [6], and the jamming gripper [7]. In such cases, a large contact area is required to generate sufficient friction, and it is typically difficult for them to grasp thin objects. Conversely, grippers belonging to the third group are good at picking up thin objects using surface adhesion, and include grippers that utilize suction [8,9], the electrostatic gripper [10], and grippers based on gecko adhesion [11,12]. Unfortunately, these grippers have difficulties handling deformable objects and objects with rough and wet surfaces. There are grippers that combine these two grasping strategies, such as the gripper combining dielectric elastomer actuator (DEA) with electro-adhesion [13], the gripper

* Corresponding author.
E-mail addresses: wangzk@fc.ritsumei.ac.jp (Z. Wang), or@isi.imi.i.u-tokyo.ac.jp (K. Or), hirai@se.ritsumei.ac.jp (S. Hirai).

https://doi.org/10.1016/j.robot.2020.103427
0921-8890/

integrating gecko adhesion onto a pneumatic actuator [14], and the gripper realizing pinch grasp and suction for delicate object manipulations [15]. However, the grippers in [13,14] do not have separable operation modes, and the gripper in [15] has a complex structure and it may be not suitable for applications in the food industry. Other types of gripper also exist for food material handling, such as the meat gripper that employs the form closure principle [16], the binding hand combining both force and form closure [17], the needle gripper [18], and the freeze gripper [19]. However, these grippers are designed for specific tasks, and they do not have multiple operation modes. Apart from robot grippers, other robots and devices take advantage of multi-mode operations, such as a dual-mode robot hand that realizes high-speed and large grasping force [20], a dual-mode sensor that has tactile and proximity-sensing capabilities [21], a walking-wheeling dual-mode humanoid robot [22], and a tri-mode sensor that performs distance measurement, motion tracking, and profile recognition [23]. They all share the same purpose of maximizing the performances by utilizing fewer resources.

According to Fantoni et al. handling systems for food products must be easy to disassemble and must withstand moisture, and the use of electronic parts should be limited [24]. Therefore, pneumatically driven systems are preferable for reasons of hygiene and system simplicity. According to [25], soft pneumatically driven actuators can be categorized into three types: ribbed, cylindrical, and pleated, based on their chamber morphologies. Among them, the pleated type has been widely adopted due to its easy fabrication and large bending range. Soft grippers consisting of multiple pleated pneumatic actuators have been applied to grasp household objects [26], perform biological sampling on deep reefs [27], and handle food materials in paper containers [28,29]. A commercial soft gripper with various applications is also described in [30]. Despite their success of grasping various objects, multi-fingered soft grippers typically exhibit difficulties grasping and handling thin and heavy objects [29]. Increasing the fingers stiffness could enhance their ability to grasp heavy weights [31], but thin objects, such as a piece of paper or a small bag of sauce, still represent a challenge for multi-fingered grippers.

In this study, we propose a dual-mode soft gripper that integrates a suction pad on the tip of each pneumatic actuator. By combining the advantages of both grasping and suction, the proposed gripper can handle a wide variety of objects. The gripper design and fabrication are introduced in Section 2, followed by finite element (FE) simulations in Section 3. Experimental validations are presented and discussed in Section 4. Section 5 presents our conclusions and future suggestions.

2. Design and fabrication

2.1. Soft finger design

The finger design and fabrication are inspired by the PneuNets actuator [32] and the soft robotics toolkit [33]. To simplify the fabrication, we eliminated the "strain-limiting layer" of PneuNets actuator, and we designed an air-paths layer to coexist the grasping and suction. When designing the soft finger, we considered the following requirements:

(1) To grasp and handle delicate and fragile objects, the finger should be as soft as possible from a structural point of view.
(2) Air paths for grasping and suction should be separated. The cross-sectional area of the suction path should be large to provide a sufficient flow rate.
(3) To adapt to different object sizes, the finger should be able to be deflated and reversely bent to a certain deformation.

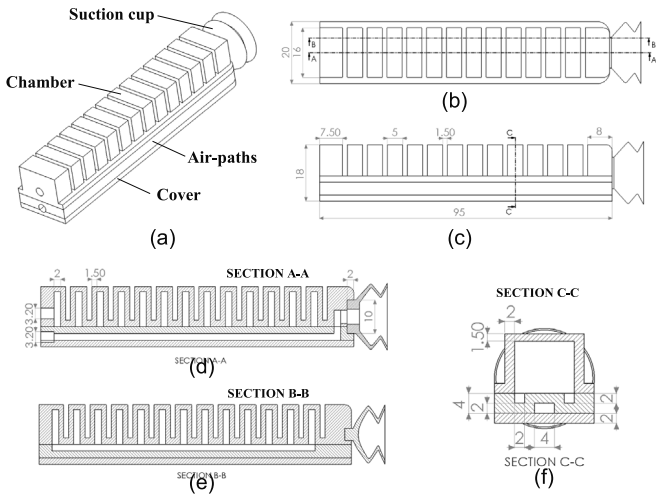

Fig. 1. Design and dimensions of the soft finger: (a) isometric view, (b) top view, (c) side view, (d) section A–A, (e) section B–B, and (f) section C–C.

(4) The finger design should facilitate casting fabrication.
(5) To avoid air leakage at the interfaces among different parts of the finger, a sufficient bonding area should be guaranteed.

After several attempts, the final design is shown in Fig. 1. The finger has dimensions of 95 mm × 20 mm × 18 mm (L × W × H) without the suction pad, which is slightly smaller than a human finger. The finger consists of four parts (Fig. 1(a)): the chamber, the air-paths, the cover, and the suction pad. As shown in Fig. 1(d) and (e), the chamber part consists of 13 air chambers and the chamber wall is 1.5 mm thick for easy inflation and deflation. The chamber cavity has a thickness of 2 mm (Fig. 1(d)). According to [34], a smaller interval between neighboring chambers yields easier bending deformation during inflation. However, it also limits the reverse bending deformation. To meet the third requirement, we set the interval to 1.5 mm (Fig. 1(c)). The air-paths consist of multiple air paths. As shown in Fig. 1(f), two air paths with a cross-sectional dimension of 2 mm × 2 mm were designed to connect all air chambers for inflation and deflation. Regarding the second requirement, the air path for connecting the suction pad was designed to have a cross-sectional dimensions of 4 mm × 2 mm. The cover part was used to seal the air path and is 2 mm thick. To satisfy the first requirement, we minimized the total thickness (6 mm) of the air-paths and cover parts. For the suction pad, we used commercial pads with one bellow because of their good performances. A circular indentation (10 mm diameter and 2 mm depth) was designed at the fingertip to position the suction pad. The CAD data of the finger design are presented and explained in the Data-in-Brief.

The chamber and cover have similar structures to those in previous research [35] and can be easily fabricated by either 3D printing or casting. The air-paths has a relatively simple structure and this enables easy fabrication of the finger and fulfills the fourth requirement. Because air leakage happens more likely during air inflation than suction, the connection of the chamber and air-paths is of great concern. To enlarge the bonding area and meet the last requirement, the chamber part was designed to have a narrow top and a wide bottom (Fig. 1(f)), and the bottom surface is 2 mm wider at each side than the top surface.

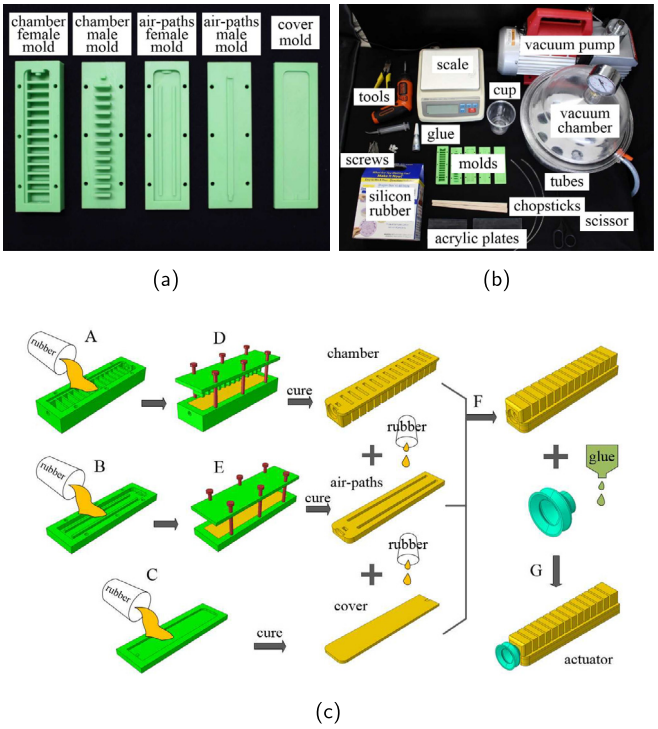

Fig. 2. Finger fabrication: (a) 3D printed molds, (b) devices and components used for casting, and (c) the fabrication process.

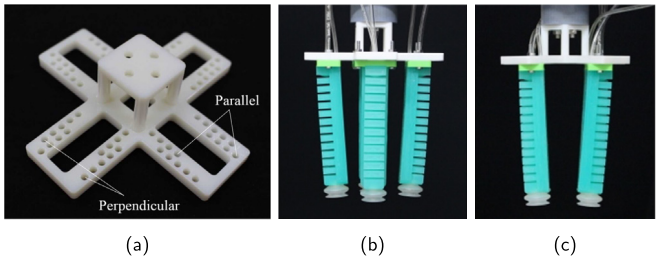

Fig. 3. Gripper base (a) and assembled grippers in (b) a perpendicular configuration and (c) a parallel configuration.

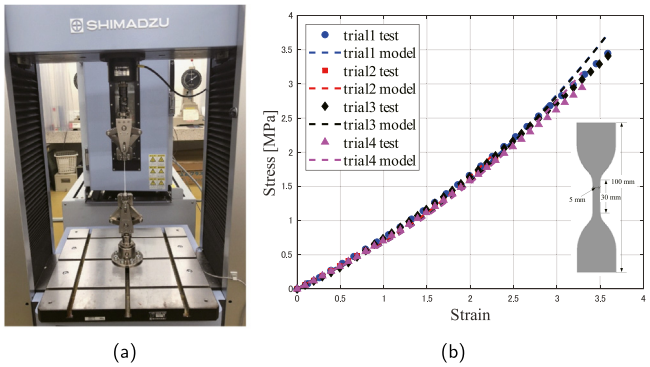

Fig. 4. Material property estimation: (a) tensile test scenario and (b) test data and model fitting.

2.2. Finger fabrication

The soft finger was fabricated following the traditional casting process. Casting molds (Fig. 2(a)) were 3D printed using a Zortrax M200 printer (Zortrax, Olsztyn). Tools and devices used for casting are shown in Fig. 2(b). Similar to [25], the fabrication process was divided into several consecutive steps as shown in Fig. 2(c). The mixed liquid rubber was first degassed for two minutes at a vacuum pressure of approximately −85 kPa. After degassing, the liquid rubber was poured into the chamber female mold (step A), the air-paths female mold (step B), and the cover mold (step C), respectively. The molds filled with liquid rubber were placed into the vacuum chamber for second degassing. Afterward, the chamber male mold and air-paths male mold were fitted into the corresponding female molds and secured with screws (steps D and E). The cover mold was sealed with an acrylic plate. After curing, the chamber, the air-paths, and the cover were carefully demolded. The three separate parts were then bonded, one on top of another, using the same liquid rubber. This completed the fabrication of the soft finger body (step F). Finally, in step G, a commercial suction pad (FGA 20 SI, Schmalz, Germany) was glued into the circular indentation at the fingertip using instant adhesive (Cemedine Co., Ltd., Tokyo). Data for 3D printing the molds and a video showing the fabrication process can be found in the Data-in-Brief.

2.3. Gripper assembly

A gripper base (Fig. 3(a)) was 3D printed using the Objet350 printer (Stratasys, MN, United States) with rigid VeroWhite material. Two series of positioning holes were designed on the base to achieve both perpendicular (Fig. 3(b)) and parallel (Fig. 3(c)) configurations of the soft fingers. A perpendicular configuration, in which the neighboring fingers are perpendicular to each other, is designed to grasp circular and square targets. In contrast, a parallel configuration is suitable for handling elongated targets because the neighboring fingers are parallel to each other. Moreover, a 5 mm gap was designed between neighboring holes to obtain adjustable opening distances between opposite soft fingers to adapt to different sized target objects. For example, the gripper in the perpendicular configuration has five different opening distances of 33 mm, 43 mm, 53 mm, 63 mm, and 73 mm, respectively. Data for 3D printing the necessary parts for gripper assembly can be also found in the Data-in-Brief.

3. Finite element simulation

3.1. Finite element model

The FE method is a relatively accurate way to reproduce the deformation behavior of deformable objects and has been frequently utilized to model and simulate soft robots [36–40]. In this study, Abaqus (SIMULIA, Dassault System, MA) was used to simulate the finger performance. Two materials, Dragon Skin 10 (DS10, Smooth-on Inc., PA) and Dragon Skin 30 (DS30), were used to model the soft finger. According to [37], DS10 can be characterized as a hyper-elastic rubber using the Yeoh model and the long-term coefficients were set to $C_{10} = 3.6 \times 10^{-2}$ MPa, $C_{20} = 2.58 \times 10^{-4}$ MPa, and $C_{30} = -5.6 \times 10^{-7}$ MPa. We performed tensile tests on the DS30 material using a tensile tester (AG-10kNXplus, Shimadzu, Kyoto). The test scenario is shown in Fig. 4(a). The dog bone sample used in the tests is shown in the inset view of Fig. 4(b). Four samples were fabricated by casting process with a thickness of 2.17 mm. During the test, the sample was fixed to the testing machine by two pantograph grips and extended at a speed of 300 mm/min until it fractured. As DS30 has a nominal elongation at rupture of 364%, the test data under

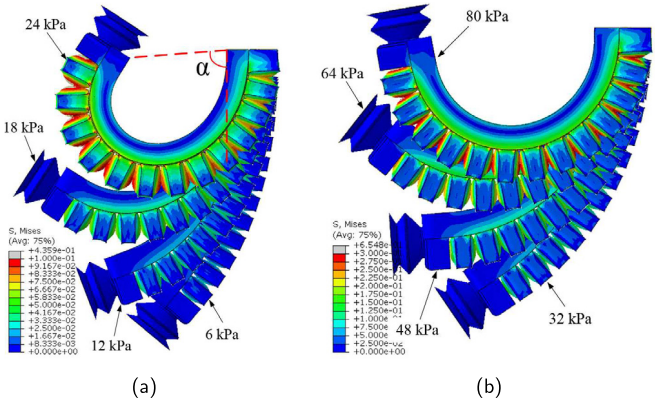

Fig. 5. Simulation results of soft finger inflation at different pressures for: (a) the finger modeled with DS10 and (b) the finger modeled with DS30.

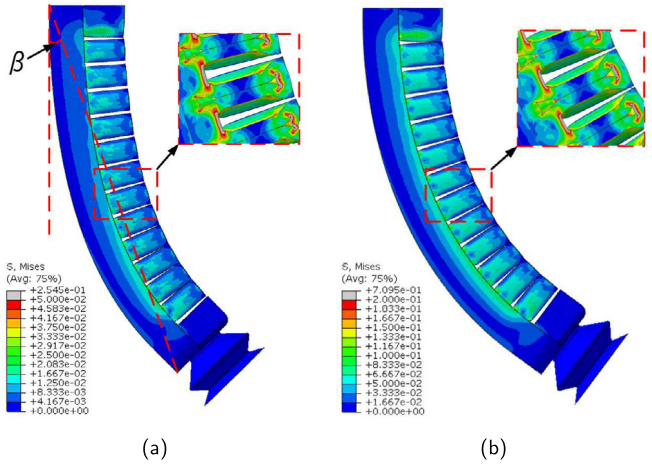

Fig. 6. Simulation results of finger deflation for: (a) the finger modeled with DS10 at a pressure of −23 kPa and (b) the finger modeled with DS30 at a pressure of −58 kPa.

360% elongation were used to estimate the material properties (Fig. 4(b)). The model estimation function of Abaqus was used to select the appropriate material model and determine the values of model parameters. Five hyper-elastic material models, the 1st-order (Mooney–Rivlin) and 2nd-order polynomial models and the 1st-order, 2nd-order, and 3rd-order Ogden models, were chosen as candidates. After model fitting, we found that only the 1st-order Ogden model generates stable results for all strains and the fitting results are shown in Fig. 4(b). The averaged material parameters are $\mu_1 = 0.2640 \pm 0.0078$ MPa, $\alpha_1 = 3.0158 \pm 0.0453$, and $D_1 = 0\,\text{MPa}^{-1}$. Raw data from the tensile tests and MATLAB programs to process the data can be found in the Data-in-Brief.

The FE model of the finger was meshed with 10-node quadratic tetrahedron hybrid elements (C3D10H) and the global mesh seed was set to 1 mm. Gravity was included in the simulations and the material densities were set to 1070 kg/m^3 for DS10 and 1080 kg/m^3 for DS30 according to the material datasheet [41]. Pressure loads (inflation, deflation, and suction) were applied on the corresponding surfaces and contact interactions were created among surfaces that contact each other. Standard/implicit simulations were conducted with geometrical nonlinearity included to account for large bending deformations. Abaqus files of the FE model can be also found in the Data-in-Brief.

3.2. Simulation of finger inflation

Simulation results of finger inflation are shown in Fig. 5. The soft finger made from DS10 material bends almost 90° (angle α in Fig. 5(a)) at a pressure of 24 kPa, and the bending curvature increases towards the suction pad end. Conversely, the finger with DS30 material reaches to 90° at a pressure of 80 kPa, and the bending curvature remains approximately constant along the finger length (Fig. 5(b)).

3.3. Simulation of finger deflation

When a negative pressure is applied, the finger can be deflated and bend in a reverse manner. This behavior was simulated by applying a negative pressure on the internal surfaces of the air chambers. For the finger modeled with DS10, FE simulation converges until a pressure of −23 kPa (Fig. 6(a)), at which the internal surfaces of the air chamber are fully contacted (inset of Fig. 6(a)). The reverse angle (β in Fig. 6(a)) is achieved at 19.24°, which was calculated using ImageJ (https://imagej.nih.gov/ij/). For the finger modeled with DS30, FE simulation converges until a pressure of −58 kPa (Fig. 6(b)) and a reverse angle of 25.89° is achieved. The finger modeled with DS10 generates a lower reverse angle because of the softness of the material. Once the internal surfaces of the air chambers reach full contact, the material stiffness plays a key role against gravity. Therefore, a stiffer material (DS30 in this comparison) can achieve a larger reverse angle.

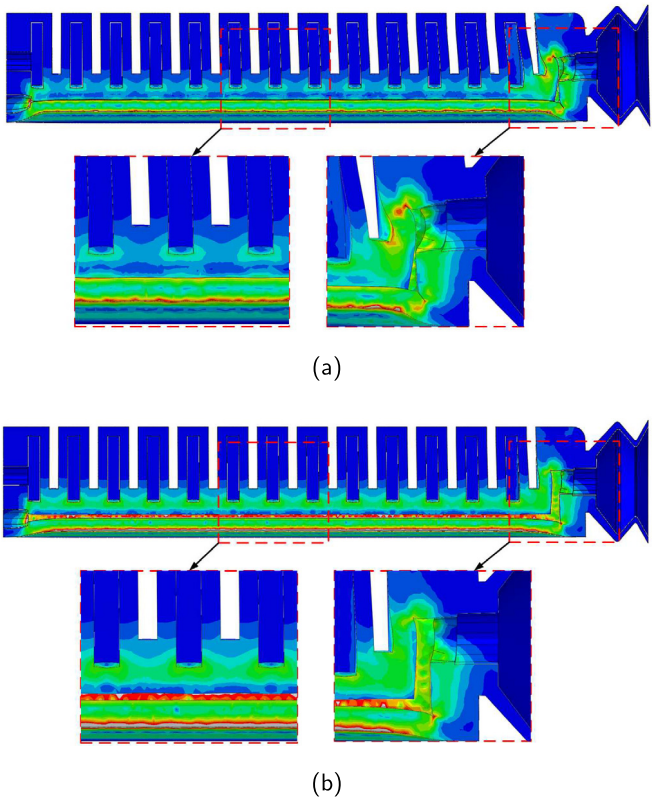

Fig. 7. Simulation results of air path suction for: (a) the finger modeled with DS10 at a pressure of −60 kPa and (b) the finger modeled with DS30 at a pressure of −90 kPa.

3.4. Simulation of air path suction

To actuate the suction pad, the air path for suction is subjected to large negative pressure. To ensure effective functionality of the air path, FE simulations were performed on the suction path. The

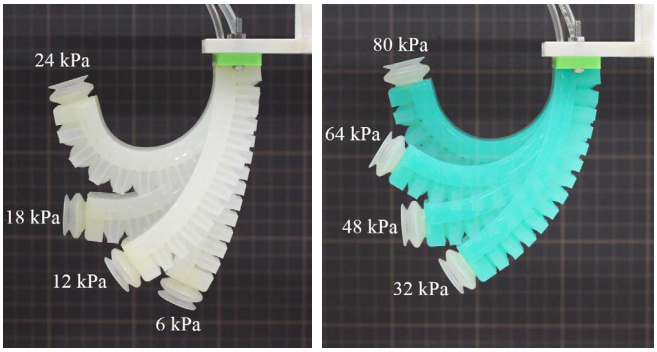

Fig. 8. Bending behaviors under different air pressures for fingers fabricated with (a) DS10 and (b) DS30 materials.

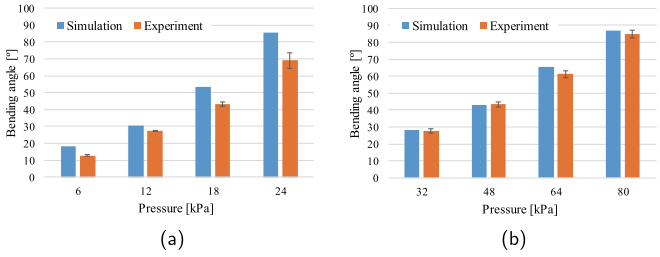

Fig. 9. Bending angle comparisons under different pressure inputs for fingers fabricated using (a) DS10 and (b) DS30 materials. Error bar indicates the standard deviation.

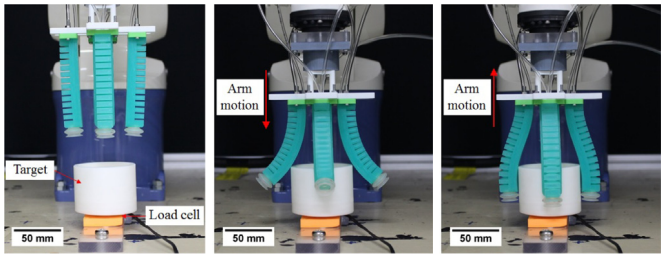

Fig. 10. Lifting force test. System setup in (a) the initial position, (b) the grasping position, and (c) the lifting position.

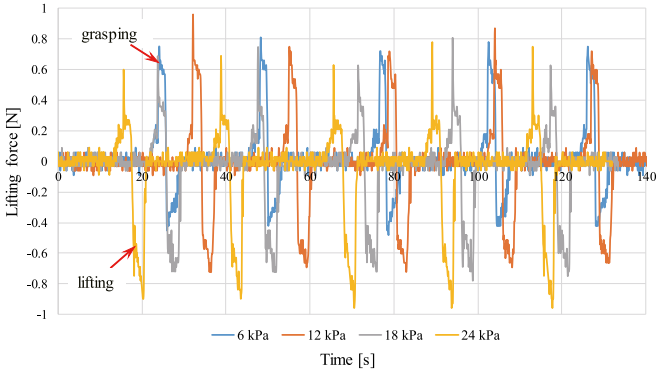

Fig. 11. Raw data of the measured lifting force for the finger fabricated with DS10 at an opening distance of 33 mm.

top surfaces of the air chambers were fixed to keep the finger straight, and a negative pressure was applied on the suction path surfaces. For the finger modeled with DS10, at a pressure of −60 kPa, the suction path at the cover side (inset view (I) in Fig. 7(a)) is completely blocked and the suction path at the fingertip side (inset view (II) in Fig. 7(a)) is almost blocked due to the softness of the material. However, for the finger modeled with DS30, the suction path is not blocked even at a pressure of −90 kPa (Fig. 7(b)).

4. Experiments

Experimental tests were performed to evaluate single finger bending, gripper lifting force, grasping and suction of various types of objects, and automatic packaging of a Japanese boxed lunch.

4.1. Single finger tests

An air compressor (JUN-AIR 3-4) and an electro-pneumatic regulator (SMC ITV2030) were used to provide constant air pressure. The same pressures used in the simulations (Fig. 5) were applied to inflate the soft fingers. Bending behaviors were recorded by a digital camera and examples are shown in Fig. 8. Four fingers fabricated using DS10 and DS30 respectively were tested to verify the individual differences among the fingers. Quantitative comparisons of bending angle between simulations and experiments are summarized in Fig. 9. For the finger fabricated using DS10, the discrepancies between simulations and experiments are relatively large. The results indicate that the material properties used in the simulation less accurately reproduce actual finger deformation; *i.e.*, the actual finger is stiffer than the simulated one. This also explains why a pressure of −60 kPa blocks the air path in the simulation (Fig. 7(a)) but not in the experiments (Section 4.4). However, the simulations and experiments agree well for the finger fabricated with DS30. In addition, individual differences among different fingers are not significant according to the standard deviations in bending angles.

4.2. Lifting force tests

To compare and demonstrate the lifting ability of the gripper for different opening distances, we performed lifting tests with force measurements. A cylindrical target (66 mm in diameter and 50 mm in length), which was 3D-printed with ABS material, was fixed on a load cell (USL06-H5-50N, Tec Gihan, Kyoto) (Fig. 10(a)) to monitor the lifting force. The soft gripper was attached to a robot arm (VP-6242, Denso, Tokyo) and the arm was programmed to perform a simple picking-up motion. At the initial position (Fig. 10(a)), the gripper was deflated to have a large opening. The gripper was then driven downward to the grasping position (Fig. 10(b)), at which the gripper was inflated to grasp the target. Then, the gripper moved upward at a speed of 390 mm/s (Fig. 10(c)). Solenoid valves (VQ110U-5M-M5, SMC, Tokyo) were used to control the on-offs for deflation and inflation. The lifting tests were performed at different pressures with different opening distances in the perpendicular configuration. The deflated gripper generated opening ranges (diameters that it can accommodate) of approximately 128.6 mm–176.9 mm and 139.5 mm–193.6 mm for the grippers fabricated using DS10 and DS30, respectively. The gripper with DS10 has a smaller opening because gravity recovers some deflation due to the softness.

Fig. 11 shows examples of the raw force data (vertical direction) for the finger fabricated with DS10 at an opening distance of 33 mm. Five trials were performed under each input pressure. The

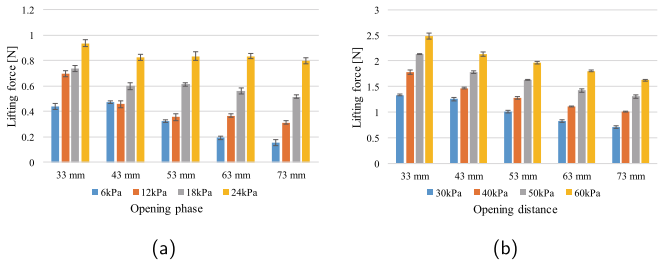

Fig. 12. Comparison of maximum lifting force for different opening distances and different materials: (a) DS10 and (b) DS30.

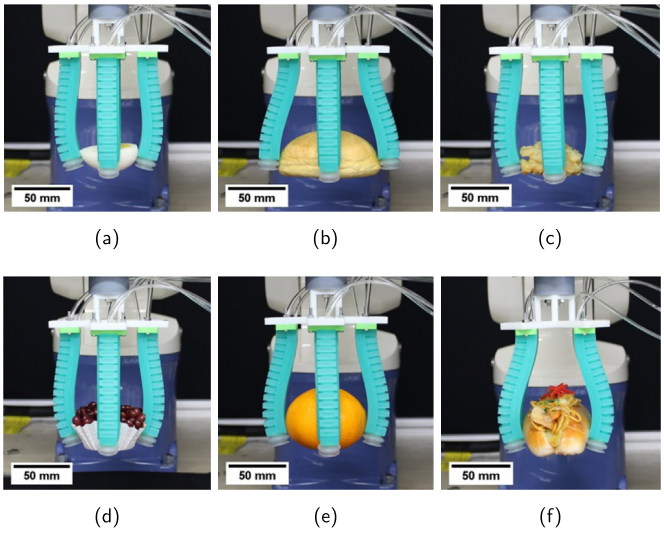

Fig. 13. Snapshots of grasping tests on: (a) half a boiled egg, (b) bread, (c) fried chicken, (d) red beans in a paper container, (e) an orange, and (f) a hot dog. (For interpretation of the references to color in this figure legend, the reader is referred to the web version of this article.)

pulses above 0 N indicate the force components when the gripper grasps the target. Pulses below 0 N indicate the lifting forces. An increase of air pressure also increases the lifting force. To quantitatively compare the differences in lifting force, we collected the maximum lifting force (absolute value) for each experimental trial as well as their average and standard deviation. Fig. 12 compares the maximum lifting force for different opening distances and different materials. It is clear that a smaller initial opening generates a larger lifting force; this trend is more apparent in the gripper fabricated with the harder material (Fig. 12(b)). This is because the smaller initial opening creates a tighter contact with the target and therefore achieves more stable grasping. A linear relationship between lifting force and air pressure is more apparent in the harder gripper (*i.e.*, comparing Fig. 12(b) with Fig. 12(a)) and the standard deviations are also smaller in Fig. 12(b) than Fig. 12(a). As a result, gripper fabricated with harder material provides more robust performance than that made of softer one.

4.3. Grasping tests

Grasping tests on various food materials were performed using the two grippers fabricated with DS10 and DS30. The grasping targets are listed in Table 1, as well as their weights and applied air pressures for lifting. The perpendicular configuration was used to grasp all targets, except the hot dog. Because of the elongated shape of the hot dog, the parallel configuration was employed. The gripper fabricated using DS10 failed to lift the hot dog, but the gripper fabricated with DS30 succeeded at a pressure of 70 kPa. Tests on other targets were successful for both grippers with various required pressures. The gripper with DS10 requires lower pressure to lift the same target, indicating that the gripper with softer fingers is more energy efficient. Fig. 13 shows grasping snapshots using the gripper with DS30. A video showing examples of grasping tests can be found in the Data-in-Brief.

Table 1
Target weights, sizes, and required air pressures (P) for grasping tests. Symbol "×" indicates failed lift.

Target	Weight [g]	Size (L × W × H) [mm]	P (DS10) [kPa]	P (DS30) [kPa]
Egg	35.46	55 × 44 × 23	15	40
Bread	26.61	97 × 58 × 43	15	40
Chicken	29.54	60 × 44 × 26	15	40
Beans	90.0	82 × 82 × 45	20	50
Orange	137.66	73 × 73 × 52	25	50
Hot dog	273.97	175 × 62 × 66	×	70

Table 2
Targets used in suction tests with their weights.

Target	Hamburger	Sauce	Rice	Kernel corn	MacBook Air
Weight [g]	80.05	100.10	254.09	512.62	1072.65

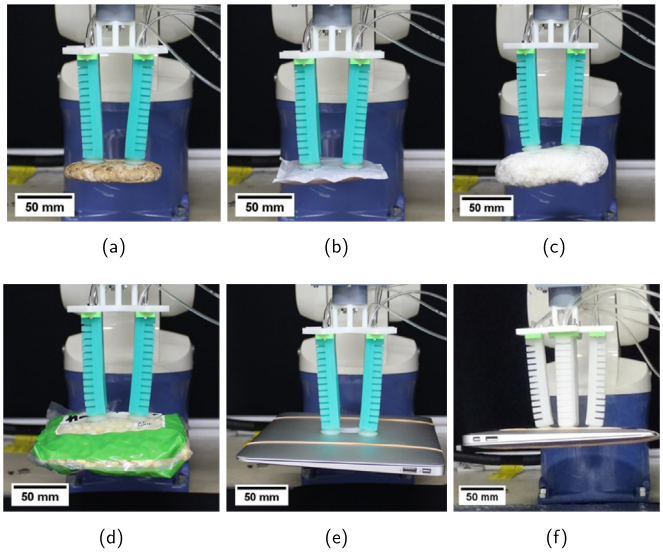

Fig. 14. Snapshots of suction tests on: (a) a frozen hamburger, (b) a bag of sauce, (c) wrapped rice, (d) a bag of kernel corn, (e) a MacBook Air using the gripper made of DS30 in parallel configuration, and (f) the same MacBook Air using the gripper made of DS10 in perpendicular configuration.

4.4. Suction tests

Suction tests on various targets were also performed using the grippers fabricated with both materials. The targets are listed in Table 2 together with their weights. The sauce and kernel corn were packaged in plastic bags. The cooked rice was wrapped in cling film. A vacuum ejector (VUE07-44A, PISCO, Japan) was used to generate negative pressure for each finger. A pressure of approximately −60 kPa and −90 kPa was used for the gripper made of DS10 and DS30, respectively, for the suction tests. All targets are lifted stably by both grippers in both finger configurations. Some snapshots of the suction tests are shown in Fig. 14. These thin and heavy targets are usually difficult to grasp. By taking the advantages of the suction pads, these targets can be successfully handled. As the suction pads on four fingers are separately

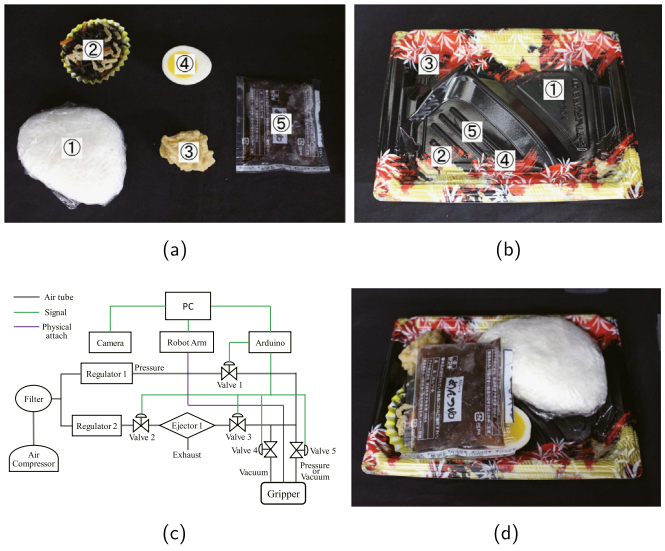

Fig. 15. Test on automatic boxed lunch packaging: (a) food materials and packaging orders denoted by circled numbers, (b) empty lunch box with circled numbers denoting the corresponding placement positions, (c) system configuration, and (d) the packaged boxed lunch.

vacuumed, the success rate is maximized. The suction pads are not only effective on smooth surfaces like the MacBook Air, but also on a frozen hamburger and plastic bags. A video showing examples of the suction tests can be found in the Data-in-Brief.

4.5. Automatic boxed lunch packaging

To demonstrate the advantages of having dual modes for the soft gripper, an automatic packaging test of a Japanese boxed lunch was conducted. The packaging food targets are shown in Fig. 15(a) with the circled number denoting the packaging order in the test. Among the targets, the wrapped rice (①) and the sauce (⑤) are relatively difficult to grasp. Therefore, the suction mode was chosen to package these two items. Conversely, the grasping mode was used for the cup of hijiki (②), the fried chicken (③), and the boiled egg (④). During the test, we assumed that the placement positions of the targets in the lunch box (Fig. 15(b)) were known; these positions are typically predetermined by human operators. Object recognition and classification approaches can be used to determine the positions and depths of the targets. Based on target information, the desired mode was chosen for the corresponding items. A robot operating system (ROS)-based system was constructed to control the packaging process, as shown in Fig. 15(c). The *Moveit* plugin is used to generate the trajectories of the robot arm. A faster region-based convolutional neural network (faster-RCNN) is used to recognize the targets, and the approximate positions of the targets are sent to the PC. Two regulators are used to set the required pressures for grasping and suction. Five valves are controlled by Arduino to realize different actions, and the switching combinations for the actions are listed in Table 3. The ROS package *rosserial* is used to establish communication between the Arduino and PC. The packaged boxed lunch is shown in Fig. 15(d). A video demonstrating the automatic packaging test can be found in the Data-in-Brief.

5. Conclusions

In the food industry, particularly small and medium-sized enterprises, high cost automation lines and complex robotic systems are difficult to introduce as simple and low-cost systems are typically required. In addition, for hygiene reasons, pneumatic driven systems are preferred. In this study, we presented a dual-mode and pneumatically driven soft gripper that combines both friction and suction principles for handling food products. Because the entire gripper was constructed using soft materials, damage to food products can be minimized during handling operations. The main contributions of this work are as follows: (1) a new dual-mode soft gripper for grasping and suction of food products was proposed; (2) a soft finger design that integrates a suction pad onto a PneuNets bending actuator and includes an effective arrangement of air paths was provided; (3) gripper capabilities were quantitatively validated through experimental tests of lifting forces at different opening distances, along with grasping and suction tests on various weighted targets; and (4) automatic packaging of a boxed lunch was shown to exhibit the advantages of using the dual-mode soft gripper.

Table 3
Switching combinations of solenoid valves for realizing different actions.

Action	Valve 1	Valve 2	Valve 3	Valve 4	Valve 5
Idle	Off	Off	On	Off	On
Inflation	On	Off	Off	Off	On
Deflation	Off	On	On	Off	On
Suction	Off	On	On	On	Off

Experiments on lifting force revealed that the soft gripper with a smaller initial opening generates a larger lifting force. The lifting force increased approximately 52.9% by shortening the initial opening from 73 mm to 33 mm at a pressure of 60 kPa using the gripper fabricated with DS30. This is because that the smaller initial opening achieves better 'wrapping' behavior and creates a tighter contact with the grasping target. Therefore, a smaller initial opening is preferable when grasping a known-sized target. Grasping tests showed that the gripper fabricated with softer materials is more energy efficient for grasping but the maximum grasping weight is lower than that fabricated with a harder material. With a pressure of 20 kPa, the gripper fabricated using DS10 can lift 90 g of red beans in a paper container. However, the gripper fabricated using DS30 requires a pressure of 50 kPa to lift the same target. Therefore, a softer gripper is preferable over a harder one as long as the target weight falls within the gripper's lifting capacity. Grasping tests also showed that the gripper can adapt to different target shapes and sizes by adjusting the initial opening and finger configurations. The gripper successfully lifted a small, ellipsoidal egg (L55 mm × W44 mm × H23 mm, 35 g) and a large, circular orange (L73 mm × W73 mm × H52 mm, 138 g) in the perpendicular configuration. By using the parallel configuration, it could lift an elongated hot dog (L175 mm × W62 mm × H66 mm, 274 g). Suction tests demonstrated that the gripper can handle a large range of targets with different weights and surface properties. The gripper could handle a 1-kg target (MacBook Air) when the surface was smooth, and it could also adapt to a moisture surface (hamburger), bagged targets (sauce and corn), and a wrapped target (cooked rice). Because the suction pad is located at the fingertip and the entire finger is flexible, the measurement of target distance can be less accurate and the gripper is more likely not to damage the target during an automatic packaging. As the vacuum suction of each finger was separately controlled, four fingers do not affect each other and success rate of target suction is maximized. Finally, the automatic packaging test showed that the proposed dual-mode gripper can facilitate automation process of food product packaging by eliminating end-effector exchange.

Due to the maximum payload (2.5 kg) of the robot arm, the maximum lifting force in suction mode was not experimentally measured. Instead, a lifting test on a MacBook Air (approximately

1 kg in weight) showed the ability of the gripper to lift heavy weights in suction mode. A lifting weight of 1 kg is large enough to handle food targets in a boxed lunch. To further enhance gripper capabilities, a mechanism for automatically switching finger configurations and adjusting opening distances will be developed in the future. Additionally, to meet the production demands of lunch box packaging, the handling efficiency of the soft gripper and system response speed will be evaluated and improved.

Declaration of competing interest

The authors declare that they have no known competing financial interests or personal relationships that could have appeared to influence the work reported in this paper.

Acknowledgments

This work was supported by the Cabinet Office (CAO), Cross-ministerial Strategic Innovation Promotion Program (SIP), "An intelligent knowledge processing infrastructure, integrating physical and virtual domains" (funding agency: NEDO).

References

[1] S. Kawamura, Expectation to future robot research for manufacturing, J. Robot. Soc. Japan 33 (5) (2015) 298–299, http://dx.doi.org/10.7210/jrsj.33.298.

[2] R. Pfeifer, F. Iida, G. Gomez, Morphological computation for adaptive behavior and cognition, Int. Congr. Ser. 1291 (2006) 22–29, http://dx.doi.org/10.1016/j.ics.2005.12.080.

[3] J. Shintake, V. Cacucciolo, D. Floreano, H. Shea, Soft robotic grippers, Adv. Mater. 30 (29) (2018) 1707035, http://dx.doi.org/10.1002/adma.201707035.

[4] K. Suzumori, S. Iikura, H. Tanaka, Development of flexible microactuator and its applications to robotic mechanisms, in: Proceedings of the 1991 IEEE International Conference on Robotics and Automation, 1991, pp. 1622–1627, http://dx.doi.org/10.1109/37.120448.

[5] Y. Chen, S. Guo, C. Li, H. Yang, L. Hao, Size recognition and adaptive grasping using an integration of actuating and sensing soft pneumatic gripper, Robot. Auton. Syst. 104 (2018) 14–24, http://dx.doi.org/10.1016/j.robot.2018.02.020.

[6] A. Pettersson, S. Davis, J.O. Gray, T.J. Dodd, T. Ohlsson, Design of a magnetorheological robot gripper for handling of delicate food products with varying shapes, J. Food Eng. 98 (2010) 332–338, http://dx.doi.org/10.1016/j.jfoodeng.2009.11.020.

[7] E. Brown, N. Rodenberg, J. Amend, A. Mozeika, E. Steltz, M.R. Zakin, H. Lipson, H.M. Jaeger, Universal robotic gripper based on the jamming of granular material, in: Proceedings of the National Academy of Sciences of the United States of America, 2010, pp. 18809–18814, http://dx.doi.org/10.1073/pnas.1003250107.

[8] S. Davis, J.O. Gray, D.G. Caldwell, An end effector based on the Bernoulli principle for handling sliced fruit and vegetables, Robot. Comput.-Integr. Manuf. 24 (2008) 249–257, http://dx.doi.org/10.1016/j.rcim.2006.11.002.

[9] T.K. Lien, P.G.G. Davis, A novel gripper for limp materials based on lateral Coanda ejectors, CIRP Ann. 57 (2008) 33–36, http://dx.doi.org/10.1016/j.cirp.2008.03.119.

[10] E.W. Schaler, D.R. III, P. Glick, V. White, A. Parness, An electrostatic gripper for flexible objects, in: Proceedings of the 2017 IEEE/RSJ International Conference on Intelligent Robots and Systems, 2017, pp. 1172–1179, http://dx.doi.org/10.1109/IROS.2017.8202289.

[11] E.W. Hawkes, D.L. Christensen, A.K. Han, H. Jiang, M.R. Cutkosky, Grasping without squeezing: shear adhesion gripper with fibrillar thin film, in: Proceedings of the 2015 IEEE International Conference on Robotics and Automation, 2015, pp. 2305–2312, http://dx.doi.org/10.1109/ICRA.2015.7139505.

[12] E.W. Hawkes, H. Jiang, M.R. Cutkosky, Three-dimensional dynamic surface grasping with dry adhesion, Int. J. Robot. Res. 35 (8) (2015) 943–958, http://dx.doi.org/10.1177/0278364915584645.

[13] J. Shintake, S. Rosset, B. Schubert, D. Floreano, H. Shea, Versatile soft grippers with intrinsic electroadhesion based on multifunctional polymer actuators, Adv. Mater. 28 (2) (2016) 231–238, http://dx.doi.org/10.1002/adma.201504264.

[14] P. Glick, S.A. Suresh, D.R. III, M. Cutkosky, M.T. Tolley, A. Parness, A soft robotic gripper with gecko-inspired adhesive, IEEE Robot. Autom. Lett. 3 (2) (2018) 903–910, http://dx.doi.org/10.1109/LRA.2018.2792688.

[15] G.P.J. Vedhagiri, A.V. Prituja, C. Li, G. Zhu, N.V. Thakor, H. Ren, Pinch grasp and suction for delicate object manipulations using modular anthropomorphic robotic gripper with soft layer enhancements, Robotics 8 (3) (2019) 67, http://dx.doi.org/10.3390/robotics8030067.

[16] Meat gripper, 2018, Available at http://www.appliedrobotics.com/products/grippers-2/pneumatic-grippers/meat-gripper/. (2018/05/28).

[17] H. Iwamasa, S. Hirai, Binding of food materials with a tension-sensitive elastic thread, in: Proceedings of the 2015 IEEE International Conference on Robotics and Automation, 2015, pp. 4298–4303, http://dx.doi.org/10.1109/ICRA.2015.7139792.

[18] T.B. Gjerstad, T.K. Lien, J.O. Buljo, Handle of non-rigid products using a compact needle gripper, in: Proceedings of the 39th CIRP International Seminar on Manufacturing Systems, 2006, pp. 145–151.

[19] T.K. Lien, T.B. Gjerstad, A new reversible thermal flow gripper for non-rigid products, Trans. N. Am. Manuf. Res. Inst. SME 36 (2008) 565–572.

[20] Y.J. Shin, H.J. Lee, K. Kim, S. Kim, A robot finger design using a dual-mode twisting mechanism to achieve high-speed motion and large grasping force, IEEE Trans. Robot. 28 (6) (2012) 1398–1405, http://dx.doi.org/10.1109/TRO.2012.2206870.

[21] H. Lee, S. Chang, E. Yoon, Dual-mode capacitive proximity sensor for robot application: implementation of tactile and proximity sensing capability on a single polymer platform using shared electrodes, IEEE Sens. J. 9 (12) (2009) 1748–1755, http://dx.doi.org/10.1109/JSEN.2009.2030660.

[22] H. Bae, I. Lee, T. Jung, J. Oh, Walking-wheeling dual mode strategy for humanoid robot, DRC-HUBO+, in: Proceedings of the 2016 IEEE/RSJ International Conference on Intelligent Robots and Systems, 2016, pp. 1342–1348, http://dx.doi.org/10.1109/IROS.2016.7759221.

[23] F. Xia, F. Campi, B. Bahreyni, Tri-mode capacitive proximity detection towards improved safety in industrial robotics, IEEE Sens. J. 18 (12) (2018) 5058–5066, http://dx.doi.org/10.1109/JSEN.2018.2832637.

[24] G. Fantoni, M. Santochi, G. Dini, K. Tracht, B. Scholz-Reiter, J. Fleischer, T.K. Lien, G. Seliger, G. Reinhart, J. Franke, H.N. Hansen, A. Verl, Grasping devices and methods in automated production processes, CIRP Ann. 63 (2014) 679–701, http://dx.doi.org/10.1016/j.cirp.2014.05.006.

[25] A.D. Marchese, R.K. Katzschmann, D. Rus, A recipe for soft fluidic elastomer robots, Soft Robot. 2 (1) (2015) 7–25, http://dx.doi.org/10.1089/soro.2014.0022.

[26] B.S. Homberg, R.K. Katzschmann, M.R. Dogar, D. Rus, Haptic identification of objects using a modular soft robotic gripper, in: Proceedings of the 2015 IEEE/RSJ International Conference on Intelligent Robots and Systems, 2015, pp. 1698–1705, http://dx.doi.org/10.1109/IROS.2015.7353596.

[27] K.C. Galloway, K.P. Becker, B. Phillips, J. Kirby, S. Licht, D. Tchernov, R.J. Wood, D.F. Gruber, Soft robotic grippers for biological sampling on deep reefs, Soft Robot. 3 (1) (2016) 23–33, http://dx.doi.org/10.1089/soro.2015.0019.

[28] Z. Wang, D.S. Chathuranga, S. Hirai, 3D printed soft gripper for automatic lunch box packing, in: Proceedings of the 2016 IEEE International Conference on Robotics and Biomimetics, 2016, pp. 503–508, http://dx.doi.org/10.1109/ROBIO.2016.7866372.

[29] Z. Wang, Y. Torigoe, S. Hirai, A prestressed soft gripper: design, modeling, fabrication, and tests for food handling, IEEE Robot. Autom. Lett. 2 (4) (2017) 1909–1916, http://dx.doi.org/10.1109/LRA.2017.2714141.

[30] Robotic systems with smart materials that unlock automation for all markets, 2018, Available at https://www.softroboticsinc.com/. (2018/05/28).

[31] Y. Li, Y. Chen, Y. Yang, Y. Wei, Passive particle jamming and its stiffening of soft robotic grippers, IEEE Trans. Robot. 33 (2) (2017) 446–455, http://dx.doi.org/10.1109/TRO.2016.2636899.

[32] F. Ilievski, A.D. Mazzeo, R.F. Shepherd, X. Chen, G.M. Whitesides, Soft robotics for chemists, Angew. Chem., Int. Ed. Engl. 50 (2011) 1890–1895, http://dx.doi.org/10.1002/anie.201006464.

[33] Soft robotics toolkit, 2019, Available at https://www.softroboticstoolkit.com/. (2019/11/08).

[34] Z. Wang, S. Hirai, Chamber dimension optimization of a bellow-type soft actuator for food material handling, in: Proceedings of the First IEEE-RAS International Conference on Soft Robotics, 2018, pp. 382–387, http://dx.doi.org/10.1109/ROBOSOFT.2018.8404949.

[35] Z. Wang, M. Zhu, S. Kawamura, S. Hirai, Comparison of different soft grippers for lunch box packaging, Robot. Biomimetics 4 (10) (2017) http://dx.doi.org/10.1186/s40638-017-0067-1.

[36] P. Polygerinos, Z. Wang, J.T.B. Overvelde, K.C. Galloway, R.J. Wood, K. Bertoldi, C.J. Walsh, Modeling of soft fiber-reinforced bending actuators, IEEE Trans. Robot. 31 (3) (2015) 778–789, http://dx.doi.org/10.1109/TRO.2015.2428504.

[37] J.H. Low, Customizable Soft Pneumatic Gripper Devices (Master's thesis), National University of Singapore, 2015.

[38] M. Manti, T. Hassan, G. Passetti, N. DÉlia, C. Laschi, M. Cianchetti, A bioinspired soft robotic gripper for adaptable and effective grasping, Soft Robot. 2 (3) (2015) 107–116, http://dx.doi.org/10.1089/soro.2015.0009.

[39] P. Moseley, J.M. Florez, H.A. Sonar, G. Agarwal, W. Curtin, J. Paik, Modeling, design, and development of soft pneumatic actuators with finite element method, Adv. Energy Mater. 18 (6) (2016) 978–988, http://dx.doi.org/10.1002/adem.201500503.
[40] Y. Hao, T. Wang, Z. Ren, Z. Gong, H. Wang, X. Yang, S. Guan, L. Wen, Modeling and experiments of a soft robotic gripper in amphibious environments, Int. J. Adv. Robot. Syst. 14 (3) (2017) 1–12, http://dx.doi.org/10.1177/1729881417707148.
[41] Dragon skin series, 2018, Available at https://www.smooth-on.com/tb/files/DRAGON_SKIN_SERIES_TB.pdf. (2018/06/04).

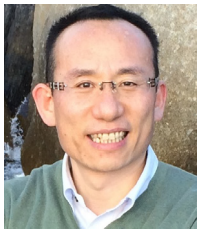

Zhongkui Wang received his Ph.D. degree in Robotics from Ritsumeikan University, Japan, in 2011. From Apr. 2011 to March 2012, he was a research associate in the Department of Robotics, Ritsumeikan University, Kusatsu, Japan. From Apr. 2012 to March 2014, he became a postdoctoral fellow at the same University. During his postdoctoral period, he visited the Swiss Federal Institute of Technology Zurich (ETHZ) for 6 months as a guest researcher. From Apr. 2014 to March 2019, he was an assistant professor in the Department of Robotics, Ritsumeikan University. Since Apr. 2019, he became associate professor at the Research Organization of Science and Technology, Ritsumeikan University. His current research interests include soft robotics, biomedical engineering, and tactile sensing.

He was the recipient of the Best Paper Award on Robotics at the 2018 IEEE International Conference on Real-time Computing and Robotics (RCAR 2018), Best Paper Award at the IEEE 24th International Conference on Mechatronics and Machine Vision in Practice (M2VIP 2017), Best Conference Paper Award Finalists at RCAR 2015 and RCAR 2017, Best Paper Award Finalist at the 2016 IEEE/SICE International Symposium on System Integration (SII 2016), and Favorite Poster Award at 2015 Simulia Community Conference.

He is a member of IEEE, Robotics Society of Japan (RSJ), Japanese Society for Nursing Science and Engineering, Japanese Society for Medical and Biological Engineering.

Keung Or received the Ph.D. degree from Waseda University, Shinjuku, Japan in 2017. From 2018 to 2019, he was a senior researcher at the Research Organization of Science and Technology, Ritsumeikan University, Kusatsu, Japan. He is currently a project researcher at the Graduate School of Information Science and Technology at The University of Tokyo, Bunkyo, Japan. His current research interests include soft robotics, robotic hand control, and tactile sensing.

He is a member of IEEE, RSJ, and Japan Society of Mechanical Engineers (JSME).

Shinichi Hirai received his B.S., M.S., and Doctoral degrees in applied mathematics and physics from Kyoto University in 1985, 1987, and 1991, respectively. He is currently a Professor in the Department of Robotics at Ritsumeikan University. He was a Visiting Researcher at Massachusetts Institute of Technology in 1989 and was an Assistant Professor at Osaka University from 1990 to 1996. His current research interests are modeling and manipulation of deformable soft objects, locomotion via deformation, and soft-fingered manipulation.

He received SICE (Society of Instrument and Control Engineers) Best Paper Award at 1990, JSME (Japan Society of Mechanical Engineers) Robotics and Mechatronics Div. Achievement Awards at 1996, the finalist of Automation Best Paper Award at 2001 IEEE Int. Conf. on Robotics and Automation, the finalist of Manipulation Best Paper Award at 2005 and 2006 IEEE Int. Conf. on Robotics and Automation, the finalist of Vision Best Paper Award at 2006 IEEE Int. Conf. on Robotics and Automation, RSJ (Robotics Society of Japan) Best Paper Award at 2008, the finalist of 2009 IEEE Int. Conf. on Robotics and Biomimetics Best Paper in Biomimetics, and the finalist of 2011 IEEE Int. Conf. on Robotics and Biomimetics Best Paper in Robotics.

He is a member of IEEE, RSJ, JSME, and Society of Instrument and Control Engineers (SICE).